

Structure of the magnetic fields in Z-pinches

G. S. Sarkisov and A. S. Shikanov

P. N. Lebedev Physics Institute, Russian Academy of Sciences, 117924 Moscow, Russia

B. Etlicher, S. Attelan, C. Rouille

LPMI, Ecole Polytechnique 91128, Palaiseau, France

V. V. Yan'kov

Russian Scientific Center "Kurchatov Institute," 123182 Moscow, Russia

(Submitted 30 March 1995)

Zh. Éksp. Teor. Fiz. **108**, 1355–1372 (October 1995)

The results are given of an experimental investigation of the spatial structure of the magnetic fields in the plasma of Z-pinches formed by the explosion of thin metallic wires used as the load of a fast high-current generator. The magnetic fields were investigated by means of the Faraday rotation of the plane of polarization of probing laser radiation at wavelength 532 nm with pulse duration 3 ns. It was shown that as the $m=0$ instability develops the current is almost completely displaced from the constriction to the periphery of the pinch (the current passing through the constriction is less than 2% of the total current through the pinch). An appreciable increase of the magnetic field in the region of the plasma plumes was observed. A rapid decrease of the magnetic field was measured at the boundary of the pinch; this indicates the presence of a return current in this region of the plasma. The results of the experiments are explained using electron magnetohydrodynamics. © 1995 American Institute of Physics.

1. INTRODUCTION

Even after several decades, there is still no flagging of the interest in Z-pinches. There are two reasons for this. First, the self-focusing of energy in the constrictions makes it possible to obtain plasma with extreme parameters, and this is exploited in many applications. Second, the self-focusing accompanying the compression of the constrictions is a most interesting physical effect in which experiment and theory reveal many new features.

From the first years of investigations to the present day, the dominant application of Z-pinches has been in controlled thermonuclear fusion.^{1–3} The more recent projects have been oriented to the attainment of maximum compression.^{4–8} Pinches play an important role as a pulsed source of neutrons.^{9–12} They are also used to generate powerful pulsed electromagnetic radiation in the range from 10 eV to 10 keV (Refs. 13 and 14). The corona of a wire exploded by the current is promising as an active medium for lasers in the range of soft x rays.⁸ All these applications require an understanding of the physics of the constrictions.

The property of energy focusing in the constrictions of Z-pinches through the development of the nonlinear stage of the $m=0$ instability mode¹⁵ was successfully used in "plasma focus" devices.^{9–11,16} To describe the self-focusing, a scaling estimate^{4,17} was proposed, derived from conservation of the current through the constriction and, therefore, from the growth in the density of the magnetic energy $\propto(I/r)^2$ during compression of the constriction. The basis of such a model is provided by two-dimensional calculations using one-fluid magnetohydrodynamics (MHD), which clearly showed the possibility of unlimited compression of

constriction.¹⁸ However, the applicability of one-fluid MHD is restricted to high linear electron densities:

$$N_e = 2\pi \int n_e r dr \gg \frac{Mc^2}{Ze^2}, \quad (1)$$

where M is the ion mass, and Z is the ion charge.

At lower linear density, the current velocity of the electrons exceeds the Alfvén velocity, and the plasma must be described, at the least, by two-fluid hydrodynamics, while the Vlasov equation gives a more accurate description. Numerical modeling of the Vlasov equation did not reveal the development of a constriction.¹⁹ However, the Vlasov equation is too complicated, and important effects in Z-pinches can be understood on the basis of a simplified description, which has become known as electron MHD.^{8,20–23} The main effects of this hydrodynamics (convection of the magnetic field by the current, the appearance of a specific resistivity) were found in theoretical studies on semiconductor plasmas, for which the ions can be regarded as fixed.^{20,21} Subsequently, it was found that a similar approximation can also be used for pinches of low linear density, $N_e < Mc^2/Ze^2$, and the explanation of the stabilization of the constriction when it reaches the boundary of the one- and two-fluid regimes became the main application to experiment.^{8,22} The stabilization was based on convective extraction of current from the constriction, but it was assumed that practically the entire pinch current remains in the constriction. Such an hypothesis agrees reasonably well with electrotechnical experimental data for pinches of high linear density. It should be noted that the strength of the magnetic field in the constriction is exceptionally important for obtaining plasma with record parameters,^{13,14,24} and therefore it is important to measure it directly.

The most informative nonintrusive method of investigating the structure of magnetic fields in a dense plasma is based on the use of the Faraday magneto-optical effect, namely, the rotation of the plane of polarization of a probing electromagnetic wave as it propagates along the magnetic field lines in the plasma. Simultaneous measurement of the distribution of the rotation angle of the plane of polarization and of the interference phase shift makes it possible to recover the spatial distribution of the magnetic field and electron density. The diagnostic method makes it possible to recover the magnetic field to an accuracy of $\approx 20\%$ with high spatial (about $5 \mu\text{m}$) and time ($\sim 1 \text{ ns}$) resolution without at the same time disturbing the plasma parameters (the flux density of the probing radiation in Faraday measurements is usually at the level $\sim 100 \text{ MW/cm}^2$). The measurements are made using a three-channel polarointerferometer, which makes it possible to observe simultaneously the Faraday, shadow, and interference images of the plasma. The method of recovering the magnetic field structure in a dense plasma is described in Ref. 25.

The Faraday rotation method was successfully used in studies to measure the space and space-time structure of magnetic fields in a laser plasma.²⁵⁻²⁹ In current systems, Faraday diagnostics was realized in "plasma focus" devices,³⁰ in a high-current Z-pinch in the Angara-5-1 facility,³¹ and also in low-induction vacuum sparks.³² However, practically all studies using Faraday diagnostics of Z-pinch have been made in the first place for the purpose of detection rather than investigation.

Our paper is arranged as follows. In Sec. 2, we describe the foundations of the method of measuring magnetic fields. In Sec. 3, we describe the facility and diagnostic complex. In Sec. 4, we give the experimental results. In Sec. 5, we give their theoretical interpretation. Finally, in the Conclusions we briefly summarize the main results of the paper.

2. THE METHOD OF MEASURING THE MAGNETIC FIELDS

The Faraday magneto-optical effect consists of a rotation of the plane of polarization of an electromagnetic wave as it propagates along the magnetic field lines in a plasma. The rotation angle is given by

$$\alpha(y) = 2.62 \cdot 10^{-17} \lambda^2 \int_0^L B_{\parallel} n_e dl, \quad (2)$$

where α is measured in radians, λ is the wavelength in centimeters, L is the path length of the probing radiation of the plasma in centimeters, B_{\parallel} is the projection of the magnetic field onto the probing direction in gauss, and n_e is the electron density per cubic centimeter. The y axis is perpendicular to the symmetry axis of the plasma. It follows from the expression (2) that in order to determine the magnetic field B it is necessary to have independent information on the electron density n_e .

To establish the distribution of the electron density, it is necessary to perform interferometry of the plasma simultaneously. The interference phase shift δ (in fringes) can be expressed in the form

$$\delta(y) = 4.46 \cdot 10^{-14} \lambda \int_0^L n_e dl. \quad (3)$$

After the distributions of the rotation angle $\alpha(y)$ and the phase shift $\delta(y)$ have been established, it is possible to recover the mean projection of the magnetic field (in kilogauss) onto the probing direction:²⁵

$$\bar{B}(y) = \frac{1.70}{\lambda} \frac{\alpha(y)}{\delta(y)}. \quad (4)$$

As was demonstrated in Ref. 25 for a Gaussian distribution of the electron density, the mean projection of the magnetic field gives a lower bound for the local magnetic field; at the same time, the form of the radial distribution of the mean magnetic field is identical to the form of the distribution of the local magnetic field. The steeper the profile of the electron density, the smaller the difference between the mean and local magnetic field. An appreciable difference between the mean and local fields is observed only if the electron density decreases toward the center of the plasma column.

In the case of an axisymmetric plasma, it is possible to recover the local distributions of the magnetic field and of the electron density by using experimentally obtained integrated distributions of the rotation angle of the plane of polarization and of the interference phase shift. Let us consider how this can be done. We represent the expressions (2) and (3) in a cylindrical coordinate system in the form

$$\alpha(y) = 5.24 \cdot 10^{-17} \lambda^2 \int_y^R \frac{B(r) n_e(r) y}{\sqrt{r^2 - y^2}} dr, \quad (5)$$

$$\delta(y) = 8.92 \cdot 10^{-14} \lambda \int_y^R \frac{n_e(r) r}{\sqrt{r^2 - y^2}} dr, \quad (6)$$

where α is measured in radians and δ in fringes.

The expressions (5) and (6) can be readily reduced to an Abel integral equation, the general form of which for axisymmetric objects is

$$S(y) = 2 \int_y^1 \frac{f(r) r}{\sqrt{r^2 - y^2}} dr. \quad (7)$$

Here and in what follows, y and r are spatial variables scaled by R . The analytic solution of the Abel equation is known as the "Abel inversion" and can be represented in two forms:

$$f(r) = -\frac{1}{\pi} \int_r^1 \frac{dS}{dy} \frac{1}{\sqrt{r^2 - y^2}} dy, \quad (8)$$

$$f(r) = -\frac{1}{\pi r} \frac{d}{dr} \int_r^1 \frac{S(y) y}{\sqrt{r^2 - y^2}} dy. \quad (9)$$

The formal transition from the expressions (5) and (6) to the Abel equation (7) can be made by using the normalized variables y and r and by writing down the appropriate expressions for $f(r)$ and $S(y)$. Thus, for the rotation angle (5) we have

$$f_B(r) = 2.62 \cdot 10^{-17} \lambda^2 R \frac{B(r)n_e(r)}{r}, \quad S_B(y) = \frac{\alpha(y)}{y}. \quad (10)$$

Accordingly, for the phase shift (6) we obtain

$$f_n(r) = 4.46 \cdot 10^{-14} \lambda R n_e(r), \quad S_n(y) = \delta(y). \quad (11)$$

Knowing the functions $f_B(r)$ and $f_n(r)$, we can write down the expression for the magnetic field $B(r)$ (in gauss) in the form

$$B(r) = \frac{1.70 \cdot 10^3}{\lambda} \frac{f_B(r)}{f_n(r)} r. \quad (12)$$

Thus, the problem of finding the spatial distribution of the field in an axisymmetric plasma reduces to determining the function $f_B(r)$ from the polarimetry and the function $f_n(r)$ from the interferometry by numerical solution of the Abel equation (7) [or one of its inversions (8)–(9)]. Methods for numerical solution of the Abel equation are now well studied and are very varied. A fairly complete review on this subject can be found in Ref. 33.

Knowledge of the local distributions of the magnetic field and of the electron density in the axisymmetric plasma makes it possible to recover the radial distributions of the current strength $I(r)$, the current density $j(r)$, and the electron drift velocity $V_d(r)$. The relationship between these parameters and $B(r)$ and $n_e(r)$ can be obtained from Maxwell's equations:

$$\begin{aligned} I(r) &= 5 \cdot 10^{-3} B(r)r, \\ j(r) &= 8 \cdot 10^{-7} \left(\frac{B}{r} + \frac{dB(r)}{dr} \right), \\ V(r) &= 6.25 \cdot 10^{18} \frac{j(r)}{n_e(r)}, \end{aligned} \quad (13)$$

where r is measured in centimeters, n_e in number per cubic centimeter, B in gauss, I in kiloamperes, j in megamperes per square centimeter, and V in centimeters per second.

The method of measuring the magnetic field structure consists of simultaneous investigation of the radial distributions of the angle of rotation of the plane of polarization and of the interference phase shift of the probing laser radiation. The angle of rotation of the plane of polarization is recovered (under the assumption of a small depolarization of the probing radiation) by means of a two-channel polarimeter. This makes it possible to avoid the errors associated with inhomogeneity of the probing beam in the transverse section and also its refraction by transverse gradients of the electron density and absorption in the plasma. It is assumed that the laser pulse is so short that the plasma parameters do not have sufficient time to change during the probing; the sign of the projection of the magnetic field vector onto the probing direction is also assumed to be constant. It is assumed that the Faraday mechanism of variation of the polarization of the electromagnetic wave predominates over the gradient mechanisms.

Let us consider this last assumption in more detail. It is well known that any anisotropy of the permittivity tensor of the plasma leads in the general case to a change in the state

of the polarization of an electromagnetic wave propagating in it. As was shown in Ref. 34, transverse gradients of the electron density can also, like the longitudinal magnetic field, have a strong influence on the change of the polarization of the electromagnetic wave. However, the experimental data published in Refs. 35 and 36 showed that if the angular aperture of the detecting optics is restricted to $\sim 10^\circ$ the detected change in the polarization of the wave is due to the Faraday effect. A strong effect of the electron density gradients on the polarization of the electromagnetic wave (mainly in the form of an increase in its ellipticity) can occur only if wide-aperture detecting optics is used in the experiment, i.e., if strongly diffracted rays are detected. This is because significant change in the polarization of the probing electromagnetic wave as a result of the transverse electron density gradients is also accompanied by appreciable refraction of the wave.

3. DESCRIPTION OF EXPERIMENT

The experiments were made using the GAEL high-current generator (Ecole Polytechnique) with the following parameters: maximum current strength ≈ 250 kA, voltage ≈ 0.5 MV, duration of current pulse ≈ 50 ns, power ≈ 0.1 TW. For probing the plasma, a powerful Nd:YAG laser with active Q switching (QUANTEL NG-24) was used. The laser consisted of a 3-nanosecond generator and three amplifiers. The energy in a pulse at wavelength $1.064 \mu\text{m}$ was ≈ 1 J. After nonlinear frequency doubling in a KDP crystal, the probing radiation had the following parameters: wavelength $0.532 \mu\text{m}$, pulse duration ≈ 3 ns, energy ≈ 250 mJ. The accuracy of the synchronization of the laser with the GAEL generator was ± 5 ns.

Figure 1 shows the optical arrangement of the three-channel polarointerferometer, which made it possible to observe and record simultaneously the Faraday, shadow, and interference images of the plasma with spatial resolution $\approx 20 \mu\text{m}$ and time resolution ≈ 3 ns (the time resolution depends on the pulse duration of the probing laser and not on the construction of the polarointerferometer). For the polarizer 3 and analyzer 13, high-quality Glan prisms with aperture $20 \times 20 \text{ mm}^2$ were used. The polarimeter contrast was about $5 \cdot 10^{-5}$, allowing the angle of rotation of the plane of polarization to be measured down to $\sim 0.1^\circ$. The difference in the aberrations of the polarimeter channels was less than 3%. For coordinate matching of the three images, the special visualizing stop 7 was used. The image of the plasma was projected by the lens 5 into the plane of the visualizing stop 7, and then the intermediate image of the plasma together with the image of the stop 7 was projected by the lens 8 onto the photodetectors in the Faraday 14, shadow 15, and interference 16 channels.

In the polarointerferometer, we used a shift polarization interferometer 12, which consisted of an entrance film polarizer, a 3° wedge made of calcite, and an exit film polarizer. The calcite wedge divides the wave incident on it into two beams and separates them in angle. Thus, in the detection plane 16 two images of the plasma shifted relative to each other in the radial direction are formed. The exit polarizer in the interferometer, causes the two beams to have the same

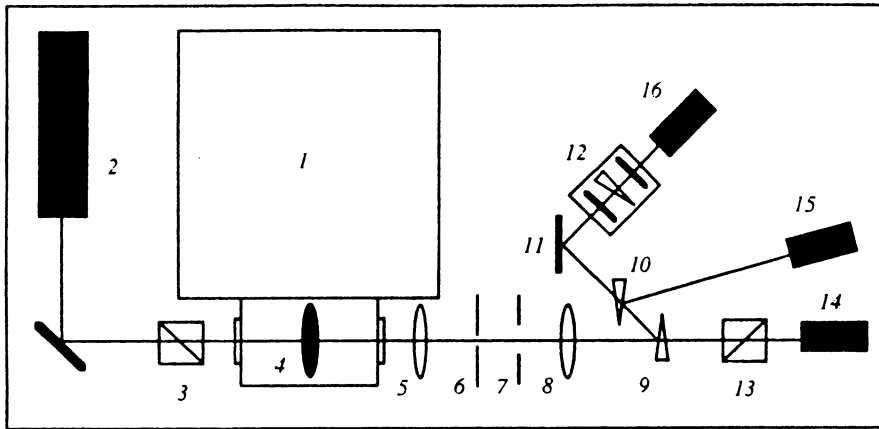


FIG. 1. Optical arrangement of three-channel polarointerferometer: 1—GAE generator; 2—Nd laser; 3, 13—Glan prisms; 4—plasma; 5, 8—lenses; 6—spatial filter; 7—visualizing stop; 9, 10—2° glass wedge; 11—100% Al mirror; 12—shift polarization interferometer (entrance polarizer—3° calcite wedge—exit polarizer); 14, 15, 16—CCD cameras of the Faraday, shadow, and interference channels.

polarization, and in the region in which they are superimposed equidistant interference fringes perpendicular to the shift direction are formed. In a number of cases, the entrance polarizer makes it possible to equalize the intensities of the interfering beams.

To reduce the self-luminosity of the plasma, we used spatial and frequency filtering. In front of the photodetector in the Faraday channel 14, we placed a narrow-band interference filter, and at the focus of the lens 5 we placed a stop 6 in the form of a narrow (~1 mm) slit. The slit was oriented perpendicular to the symmetry axis of the pinch. This made it possible to let through the stop laser radiation that had not undergone refraction and also radiation that had undergone refraction perpendicular to the symmetry axis of the pinch, along which the macroscopic gradients of the electron density were directed. At the same time, the radiation of the plasma itself did not have a preferred direction in space, and therefore was not focused in the plane 6; this caused the slit stop to reduce it substantially.

As photodetectors, we used three CCD cameras with optic fiber input (Philips NXA 1050/50). We developed a special electronic pulse distributor to ensure synchronization of the laser pulse with the time of firing of the CCD cameras. The signals from the CCD cameras were sent to the buffer memory of individual controller cards in a PC-286 personal computer and then transferred to the hard disk in the TIFF format. Before this, the CCD cameras were calibrated in the light of the probing laser using a 9-step neutral optical attenuator.

Special computer programs were written for the determination of the rotation angle of the plane of polarization, the interference phase shift, the magnetic field strength, the electron density, and also the other plasma parameters. The rotation angle of the plane of polarization was recovered by comparing the change of the relative intensities in corresponding sections of the Faraday and shadow channels. The accuracy in the measurement of the rotation angle reached ~0.1°. The measurement errors were largely determined by the contrast of the polarimeter and uncorrelated interference modulation in the Faraday and shadow channels associated with the high degree of coherence of the laser radiation. The differential method was also used to recover the interference phase shift. The coordinates of the maxima and minima of the interference fringes in the corresponding sections of the perturbed and unperturbed (obtained directly before firing the device) interferograms were compared. In such an approach, the accuracy in the measurement of the phase shift reached ~0.05 of a fringe. The recovered distributions of the rotation angle and the phase shift were then smoothed and used to construct the local distributions of the magnetic field, the electron density, the current strength, the current density, and the other plasma parameters. Performing such an analysis in different sections of the image of the plasma yields the two-dimensional distribution of the plasma parameters.

4. RESULTS OF THE EXPERIMENT

As the load in the experiments, we used thin metallic wires of different materials (Al, Cu, Ta) of diameter 20–25



FIG. 2. Faraday (a), shadow (b), and interference (c) images of plasma formed by the explosion of a 25-micron Al wire. The image was obtained 55 ns after the beginning of the current and 13 ns before the beginning of the x-ray emission. The current strength at the probing time was ~100 kA.

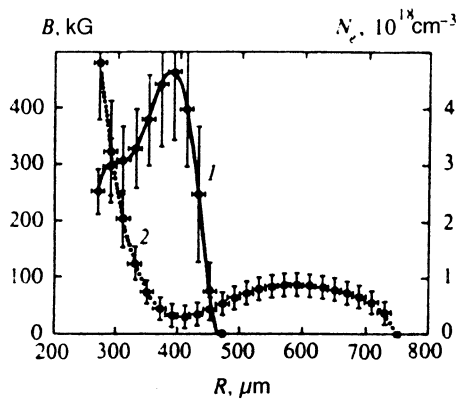


FIG. 3. Radial distribution of the magnetic field induction (curve 1) and electron density (curve 2) in section *a* identified in Fig. 2.

μm and length 10 mm placed in the cathode–anode gap of the GAEL high-current generator. Simultaneously, by means of a set of five *pin* diodes placed behind different filters, we investigated the time dependence of the x-ray emission. In each firing of the equipment, we measured the time profile of the current (by means of an induction loop placed in a return conductor) and the time of arrival of the probing laser radiation at the pinch plasma (by means of a high-speed pin diode). In our experiments, the characteristic values of the rotation angle of the plane of polarization and of the interference phase shift of the probing radiation with wavelength 532 nm were $\approx 0.5^\circ$ and $\approx 2\pi$, respectively.

4.1 Measurement of the magnetic field in the constriction of a Z-pinch

Figure 2 shows the Faraday (a), shadow (b), and interference (c) images of the plasma produced by the explosion of a 25-micron aluminum wire. The probing was done 55 ns after the beginning of the current (allowing around 40 ns for the prepulse of the device) and approximately 13 ns before the start of the x-ray emission. According to the data of the induction sensor, the current strength at this time was ~ 100 kA. In the image, one can see a well-developed constriction (section *b*). An appreciable Faraday effect was observed in the region of the plasma plumes, but our attention will be directed to the region of the constriction—sections *a* and *b*, which are separated by 100 μm .

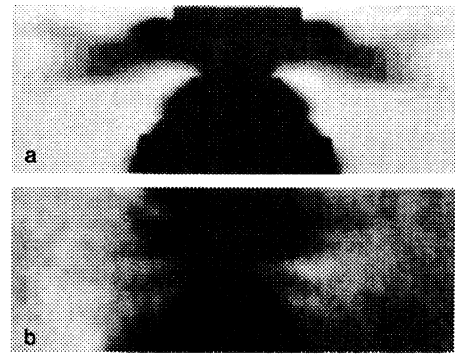


FIG. 5. Two-dimensional distribution of the interference phase shift in the region of the constriction (a) and the corresponding fragment of the shadow image (b).

The distributions of the magnetic field and of the electron density in section *a* are shown in Fig. 3. At distance 400 μm from the pinch axis, the magnetic field reaches ≈ 460 kG (corresponding to a current ≈ 90 kA). The electron density has a maximum of $\approx 5 \cdot 10^{18} \text{ cm}^{-3}$ near the opacity boundary (at distance $\approx 280 \mu\text{m}$ from the center) and then rapidly decreases toward the periphery.

Figure 4 shows the distributions of the interference phase shift (a) and of the rotation angle of the plane of polarization (b) in section *b*, which directly corresponds to the region of the constriction (see Fig. 2). Although it was possible to measure reliably the interference phase shift at the level of ≈ 0.3 of a fringe (corresponding to an electron density $\approx 5 \cdot 10^{18} \text{ cm}^{-3}$ at $\approx 50 \mu\text{m}$ from the center of the pinch), the distribution of the rotation angle of the plane of polarization clearly has a noisy dependence with amplitude $\approx 0.05^\circ$. The reliable measurement of the phase shift (to ≈ 0.05 of a fringe) makes it possible to give an upper bound for the mean magnetic field at $\approx 50 \mu\text{m}$ from the center of the pinch (the boundary of the opaque region): $B < 80$ kG, which corresponds to a current $I < 2$ kA. This is less than 2% of the total current through the pinch at the time of probing.

At the same time, as can be seen in Fig. 5b (a fragment of the shadow image of the pinch in Fig. 2), a slight plasma plume can be observed in the region immediately next to the pinch. At the same position in the interferogram, one can see the occurrence of a small disturbance of the interference

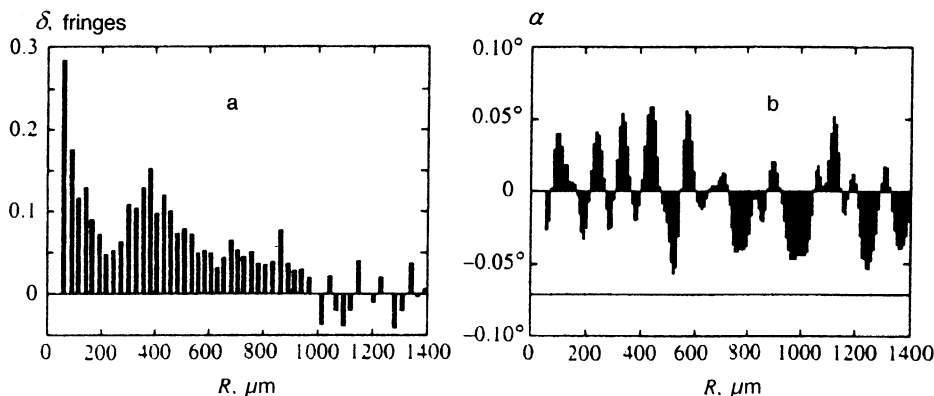


FIG. 4. Radial distribution of the interference phase shift (a) and of the rotation angle of the plane of polarization (b) in section *b* identified in Fig. 2.

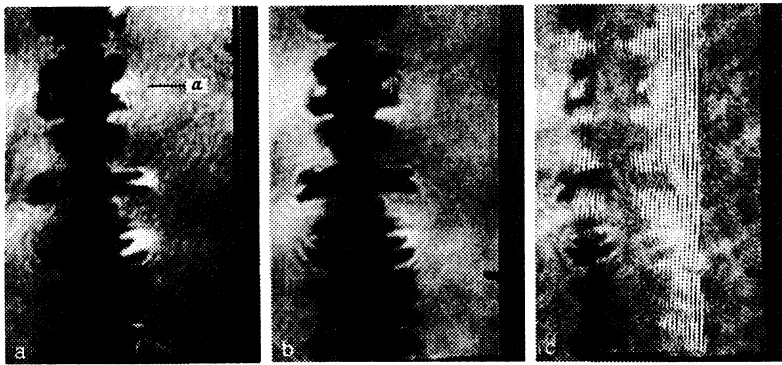


FIG. 6. Faraday (a), shadow (b), and interference (c) images of plasma formed by the explosion of a 25-micron Ta wire. The image was obtained 70 ns after the beginning of the current and 17 ns before the beginning of x-ray emission. The current strength at the time of probing was ≈ 190 kA.

fringes that is directed toward the periphery of the pinch. Figure 5a shows the two-dimensional distribution of the interference phase shift recovered by analyzing 11 radial sections in the interferogram at intervals of $25 \mu\text{m}$. It can be seen clearly in the image that as the constriction forms a radial ejection of plasma to the periphery of the pinch occurs in the neighboring region. A similar picture was observed in many firings in which a constriction could be detected.

4.2 Structure of the magnetic field in the region of the plasma plumes

Figure 6 shows the Faraday (a), shadow (b), and interference (c) images of the plasma formed by the explosion of a 25-micron Ta wire. The probing was done 70 ns after the start of the current and ≈ 17 ns before the beginning of the x-ray emission. The current strength at this time was ≈ 190 kA. In the Faraday image, it can be seen that there is an appreciable magneto-optical effect in the region of the plasma plumes, which have the shape of a disk with double rim.

Figure 7 shows the radial distribution of the magnetic field and the electron density in section *a* in the region of the plasma plumes. The magnetic field was observed to rise rapidly to ≈ 2.2 MG and then to decay as rapidly. The electron density also increased to $\approx 2.1 \cdot 10^{19} \text{ cm}^{-3}$ and then decayed. It is interesting to note that in the region in which the magnetic field has a maximum the electron density has a minimum, while in the region of a maximum of the electron

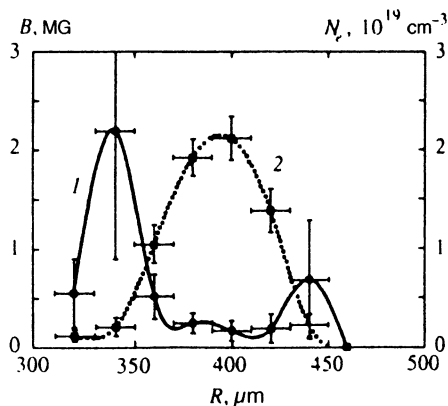


FIG. 7. Radial distribution of the magnetic field induction (curve 1) and of the electron density (curve 2) in section *a* identified in Fig. 6.

density the magnetic field is minimal. Despite the appreciable errors of the measurements, the presence of a sharp maximum of the magnetic field $340 \mu\text{m}$ from the center of the pinch is an experimental fact and is confirmed by the circumstance that in this region the measured rotation angle of the plane of polarization has a maximum while the interference phase shift has a minimum.

4.3 Distribution of the magnetic field at the boundary of the Z-pinch

We now consider the distribution of the magnetic field at the boundary of the pinch. Figure 8 shows the Faraday (a), shadow (b), and interference (c) images of the plasma formed by the explosion of a 20-micron Ta wire. The probing was done 30 ns after the beginning of the current and ≈ 40 ns before the beginning of the x-ray emission. The current strength at this time was approximately 55 kA. In this shot, the $m=0$ instability mode had not yet succeeded in developing, and it proved to be possible to measure the Faraday effect at the boundary of the Z pinch in section *a* (and not in the plasma plumes, as in Fig. 6).

Figure 9a shows the radial distributions of the magnetic field induction and of the electron density in section *a*. The magnetic field induction reaches a maximum of ≈ 300 kG at $\approx 410 \mu\text{m}$ from the center of the pinch and then decays. The electron density decreases from the value $\approx 3 \cdot 10^{19} \text{ cm}^{-3}$ at the boundary of the opaque region ($\approx 340 \mu\text{m}$ from the center) toward the periphery of the pinch. The most interesting result is the fact that magnetic field decreases radially much more strongly than $\sim 1/r$, indicating the presence of a return current in the peripheral region of the Z-pinch. Figure 9b shows the radial distributions of the current strength and the current density in section *a*. The current reaches a maximum value ≈ 60 kA at $\approx 410 \mu\text{m}$ from the center of the pinch; this agrees to within 20% with the data of the electrotechnical measurements. The current density has a maximum of approximately 35 MA/cm^2 near the region of opacity and then decreases rapidly and changes sign at the pinch periphery. The large errors in reconstructing the magnetic field at the pinch periphery are due to the decrease in this region of the detectable values of the rotation angle of the plane of polarization and of the interference phase shift. However, this does not affect the conclusion that there is a return current at

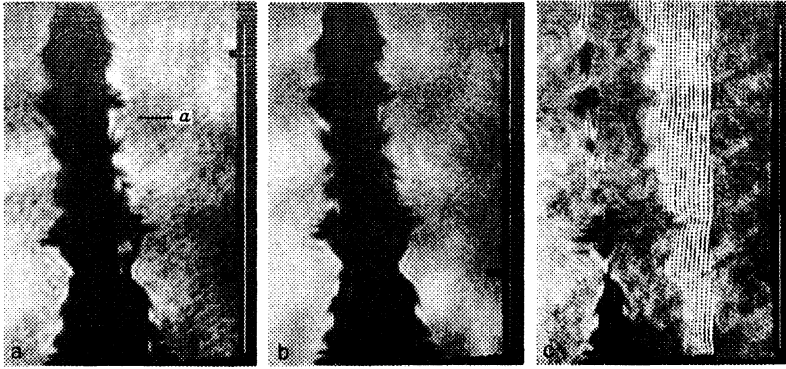


FIG. 8. Faraday (a), shadow (b), and interference (c) images of the plasma formed by explosion of 20-micron Ta wire. The image was obtained 30 ns after the beginning of the current and 40 ns before the beginning of the x-ray emission. The current strength at the time of probing was ≈ 55 kA.

the boundary of the Z-pinch. Only the absolute magnitude of the reverse current is in doubt.

5. DISCUSSION OF THE RESULTS OF THE EXPERIMENTS

5.1 Magnetic field in the pinch

There is no doubt that the most remarkable result of the experiments is the almost complete loss of current from the constriction (the current through the constriction is less than 2% of the total current through the pinch). Such a picture contradicts the standard one-fluid scenario. Analytical solutions describing a wave of current loss from the restriction to the periphery of the pinch by means of two-fluid MHD were given in Ref. 37, but the reason for the occurrence of resistance near the axis was not completely clear. A natural explanation of the experiment can be given on the basis of electron MHD. The description is simplest if one ignores current dissipation and the generation of magnetic fields by the thermal pressure of the electrons. In this case, the magnetic field is frozen into the electrons, and important results can be obtained by using just the conservation laws.

We shall assume that the electron line density corresponds to the condition of applicability (1) of electron MHD, this corresponding in our experiments to the inequality

$$5 \cdot 10^{12} \text{ cm}^{-1} \approx \frac{mc^2}{2e^2} \ll N_e \ll \frac{Mc^2}{2Ze^2} \approx 1.8 \cdot 10^{17} \text{ cm}^{-1}. \quad (14)$$

For an estimate, we have here substituted doubly ionized aluminum. In accordance with the results of the interference measurements,³⁸ the linear density of the electrons in the

region of the constriction is close to 10^{15} cm^{-1} , and this corresponds precisely to the region of applicability of electron MHD. We consider a stationary axisymmetric flow of electrons in the constriction and a tube of force lines of the magnetic field with small cross section S . Then conservation of the magnetic flux means that

$$BS = \text{const}. \quad (15)$$

When the tube is convected by the electron current to a new position, the total current within the tube is conserved:

$$I \propto Br = \text{const}, \quad (16)$$

where r is the distance to the axis of the pinch. It is this conservation law that ignores the current of the ions and corresponds to the approximation of electron MHD. The final, third conservation law corresponds to quasineutrality and to conservation of the number of electrons within the given magnetic tube:

$$2\pi r S n_e = \text{const} \quad (17)$$

Eliminating S and B from the three equations (15)–(17), we find that the current flows along the lines $n_e r^2 = \text{const}$:

$$I = I(n_e r^2). \quad (18)$$

This simple and important result was obtained in Refs. 20 and 21 for the plasma of semiconductors, and in Ref. 22 it was derived from the conservation laws, and the conditions were found under which it is possible to ignore the ion-acoustic resistance, the ion current, and the generation of magnetic fields in the plasma of the constriction. The result was also independently obtained in Ref. 39. From (18) there

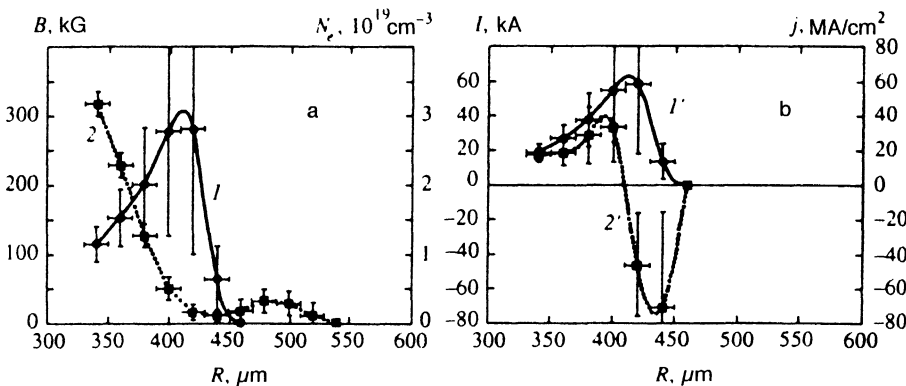


FIG. 9. Radial distribution of the magnetic field induction (I) and of the electron density (2) (a), and also of the current strength (I') and of the current density ($2'$) (b) in the section a identified in Fig. 8.

follows conservation of the linea density of the electrons along the streamlines, and this contradicts an outflow of plasma along the constrictions, as a result of which it could be conjectured that the constrictions cease to develop when they reach the boundary of applicability of ordinary MHD and electron MHD.²² In a more physical form, this important consequence means stabilization of the constrictions when the current velocity is increased to a value of the order of the Alfvén velocity. Stabilization of the constriction at these parameter values does indeed occur in experiments with different types of pinch; moreover, the constrictions survive in the stabilized state for ~ 100 MHD-times (see the review of Ref. 8).

In our experiment, the electron linea density was initially small, while the current velocity of the electrons was not small compared with the Alfvén velocity, and therefore the scenario described above must at the least be modified. However, the reason for the disappearance of the current from the constriction can be stated at once: Since the interferometry shows a low electron linea density in the constriction, the current will be displaced from it in accordance with electron MHD and the expression (18).

However, after this a difficult question arises. If there is no current in the constriction, why did the constriction arise? The theory predicted removal of the current,^{22,23} but it was tacitly assumed that such a constriction must not arise. To explain our experiments, it is necessary to consider a new mechanism. Here, the experience gained from investigation of near relations of Z-pinches—plasma opening switches^{40–45} is helpful. The opening switches usually consist of two coaxial cylinders, the gap between which is filled with plasma. They possess axial symmetry, like Z-pinches, and in both types of device there is an explosive growth of the electrical resistivity, though the subsequent evolution is different.

In the opening switches, the current is transferred along the coaxial channel to the useful load, but in pinches there is nowhere for the current to be transferred, and it continues to flow in the constriction with a possible displacement to its outer part. Roughly speaking, an opening switch is a Z-pinch in which the inner part consists of metal, and therefore compression of the current to the axis is forbidden but an explosive growth of the resistivity nevertheless occurs for some reason. This phenomenon was discovered and successfully used to peak the power in experiments.^{40,41} As the reason for the current breaking, growth of the vacuum gap near the cathode was suggested; direct experimental information about the opening mechanism was not available. Reference 42 proposed an alternative theory of the effect on the basis of a specific electron MHD resistance that was originally developed for pinches.^{8,20,21} It is convenient to represent this resistance (in ohms) in the form^{23,42}

$$R = 15 \frac{u}{c}, \quad (19)$$

where $u = I/(\pi r^2 n_e e)$ is the analog of the mean current velocity. Physically, this resistance corresponds to dissipation of the characteristic energy flux $W = uB^2/8\pi$, and in the language of forces it corresponds to the loss by each electron of

its electromagnetic momentum $\mathbf{p} = e\mathbf{A}/c$, where \mathbf{A} is the vector potential of the magnetic field. As can be seen from the expression (19), the decrease of the linea density causes the resistance of the plasma to rise long before the loss of quasineutrality, which occurs at a current velocity of the order of the velocity of light. The growth in the resistance due to the decrease in the linea density gives rise to heating and expansion of the plasma with an explosive growth of the resistance. The qualitative theory of opening switches on the basis of electron MHD found confirmation in the numerical modeling of Ref. 43, and later in the experiments of Ref. 44; additions to the theory were made in Ref. 45.

To explain the development of the constrictions under the conditions of low linea density, it is sufficient to use the form of the theory of opening switches of Ref. 45, reserving, however, the possibility of a strong change of the current radius, this reducing in practice to replacement of the expression “density” by the expression “linea density.”

Thus, the constriction develops not so much as a result of growth of the magnetic pressure due to compression, as in ordinary pinches of high linea density, but as a result of the growth of the electrical resistance and a thermal explosion. In the final stage, the current is transferred to the outer part of the pinch corona.

5.2 Magnetic field in the region of the plasma plumes

An interesting feature is also the observation at the rim of the plasma plumes of magnetic fields with pressure exceeding by an order of magnitude the pressure corresponding to the total current through the pinch.

For this, there can be several explanations. For example, if axial symmetry is lost, the standard procedure for recovering the local plasma parameters by solving Abel equations can lead to overestimated results. However, analysis of the experimental data does not confirm this hypothesis. Another possibility is associated with compression of the plasma and freezing of the magnetic field by shock waves; however, these must be two ultrastrong shock waves, which is very improbable.

The most natural mechanism appears to be one well known in a laser plasma, namely, the generation of magnetic fields by nonparallel gradients of the temperature and density (thermoelectric power mechanism). If the nonlinearity with respect to the magnetic field and the dissipation are ignored, the generation equation has the simple form

$$\frac{\partial B}{\partial t} = 100 \nabla T_e \frac{\nabla n_e}{n_e}, \quad (20)$$

where B is measured in megagauss, the distance in centimeters, and T_e in electron volts. For our conditions, taking perpendicular gradients, characteristic distance $\approx 50 \mu\text{m}$, time ≈ 10 ns, and temperature ≈ 25 eV, we obtain a field ≈ 1 MG, while the measured field is approximately twice as large [see the radial profile $B(r)$ in Fig. 7]. Of course, for the generation of such strong fields the thermal energy density must be appreciable, and therefore we recall that the greatest thermal energy density in pinches can be attained in the dense plasma

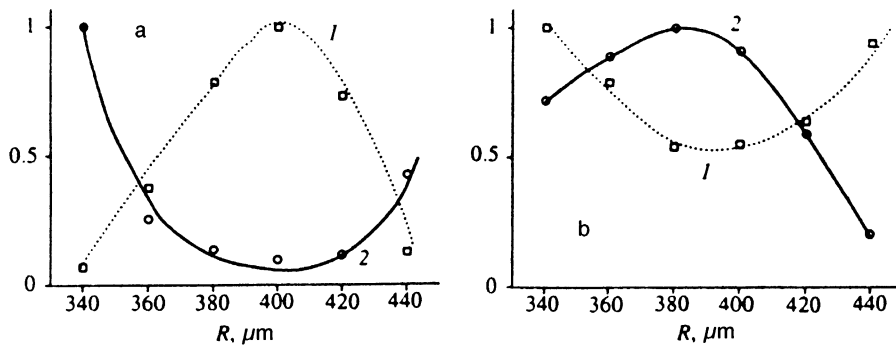


FIG. 10. Distributions of the parameters $n_e r^2$ (1) and Br (2) constructed for the radial distributions of the electron density $n_e(r)$ and the magnetic field induction $B(r)$ shown in Fig. 7(a) and in Fig. 3(b).

next to the constriction. This plasma is heated by contact with the much hotter and less dense plasma of the corona of the restriction.

5.3 Magnetic field at the boundary of the Z-pinch

Finally, the measurements of the magnetic fields at the boundary of the Z-pinch (section *a* in Fig. 8) show the appearance of strong reverse currents. Such currents are no novelty even in cylindrical pinches,⁴⁶ and they also appear entirely naturally in the presence of plasma flow around the constriction,⁴ which may possibly have been observed in section *a* in Fig. 2.

In our case, the reverse currents make possible a direct verification of the freezing-in law in electron MHD. In accordance with expression (18), this possibility is based on flow of a stationary current along the lines $n_e r^2 = \text{const}$. If the line $n_e r^2 = \text{const}$ passes through a given section twice, expression (18) can be verified. Let us consider the distributions of the electron density of the plasma and the magnetic field shown in Figs. 3 and 7. Figure 10a gives the distributions of the parameters $n_e r^2$ and Br corresponding to the radial distributions $n_e(r)$ and $B(r)$ in Fig. 7. The extrema of $n_e r^2$ and Br coincide to good accuracy. Figure 10b gives the distributions of $n_e r^2$ and Br corresponding to Fig. 3. As in the previous case, coincidence of the extrema (but "out of phase") is observed. It can be seen that equal values of the current Br correspond to nearly equal values of the local linear density $n_e r^2$. It is very probable that the lines $n_e r^2 = \text{const}$, moving along the axis of the pinch, turn round and intersect the investigated section *a* second time. The streamlines turn round and intersect the section *a* second time too, and this leads to the formation of a reverse current channel and, accordingly, to a rapid (faster than $1/r$) decay of the magnetic field at the boundary of the Z-pinch. Thus, the dependence (18), which is fundamental for electron MHD, has been experimentally verified for the first time.

Of course, in neither case is complete symmetry of the branches observed. This can be explained by the growth of the errors at the periphery of the plasma (associated with the decrease in the values of the rotation angle of the plane of polarization and the interference phase shift that can be detected in the experiment). Physical factors also cause the streamlines of Br to deviate from the lines $n_e r^2 = \text{const}$. First, there is generation of magnetic field by nonparallel temperature and density gradients; second, there is the electrical re-

distance; third, there is motion of the ions and nonstationarity of the electron flow. In our experiments, we cannot unambiguously say which of these factors is the most important.

6. CONCLUSIONS

Our measurements of the spatial structure of the magnetic fields in a Z-pinch have made it possible to discover new effects in the constrictions. This was made possible by our operating in the new range of low linear electron densities. Despite the small radius of the pinch in the region of the constriction, it was possible in the experiment to observe a fairly large (for probing at the wavelength $\lambda = 532$ nm) interference phase shift.

These effects admit a natural explanation in the framework of electron MHD. The effect of current loss from the constriction (according to the results of the measurements, less than 2% of the total current through the pinch remains in it) can be explained by convective transfer of current and the sharp growth of the electron MHD resistance. A similar process apparently occurs in plasma opening switches. The simultaneous measurements of the spatial distribution of the magnetic field induction and of the electron density made in the range of low linear densities made it possible to verify for the first time the fundamental law (18) of electron MHD. This law is used in many theoretical studies. Of course, this is a preliminary result. Nevertheless, it may be hoped that in subsequent experiments Faraday diagnostics of the pinch will make it possible to recover the two-dimensional pattern of the streamlines. It is difficult to overestimate the importance of such measurements for the theory of electron MHD.

We have actually found a range of plasma parameters that is amenable to laser diagnostics and at the same time can be described by electron MHD, which differs appreciably from ordinary MHD. The fragmentary detection of the Faraday magneto-optical effect in the experiments with Z-pinch apparently indicates that the method is insufficiently sensitive at the wavelength 532 nm, and therefore suggests that it would be promising to probe the plasma in the infrared wavelength range. It may be hoped that further experiments in this direction will give much new information about the physics of Z-pinch. In the first place, the questions of interest are 1) whether the effect of redistribution of the current from the constriction to the periphery is a universal property of Z-pinch (plasma focus, liner systems, vacuum sparks, etc.) or occurs only in pinches with low lin-

ear densities in the region of the constriction and 2) what is the role in the dynamics of formation of the Z-pinch of the low-density plasma surrounding it.

There may be effects associated with depolarization of the probing radiation (because of birefringence or anisotropy of the absorption of circularly polarized electromagnetic waves) and also with the presence in the pinch of a filamentary structure of both the current and the electron density, which may affect the results of the experiments. However, this is a subject for separate investigations.

The work reported here was done mainly under the contracts EC#SC1*-CT91-0728, ETCA/CEG #420/115/01, and DRET #92/134, and was also partly supported by the International Science Foundation (Grant No. MM1000) and the Russian Fund for Fundamental Research (Grant No. 94-02-03864-a).

- ¹L. A. Artsimovich, A. M. Andrianov, O. N. Bazilevskaya *et al.*, *At. Energ.* **3**, 76 (1956).
- ²O. A. Anderson, W. R. Baker, S. A. Colgate *et al.*, *Phys. Rev.* **109**, 612 (1958).
- ³S. Yu. Luk'yanov, *Hot Plasma and Controlled Thermonuclear Fusion* [in Russian] (Nauka, Moscow, 1975).
- ⁴V. V. Vikhrev and S. I. Braginskii, in *Reviews of Plasma Physics*, Vol. 10, ed. by M. A. Leontovich Consultants Bureau, New York (1986).
- ⁵J. W. Shearer, *Phys. Fluids* **19**, 1426 (1976).
- ⁶M. G. Haines, M. Coppins, and I. D. Culverwell, in *Proc. Second International Conference on Dense Z-Pinches*, ed. by N. R. Pereira, J. Davis, and N. Rostoker, AIP, Laguna Beach, 1989, p. 203.
- ⁷A. E. Robson, in *Proc. Second International Conference on Dense Z-Pinches*, ed. by N. R. Pereira, J. Davis and N. Rostoker, AIP, Laguna Beach, 1989, p. 362.
- ⁸V. V. Yan'kov, *Fiz. Plazmy* **17**, 521 (1991) [*Sov. J. Plasma Phys.* **17**, 305 (1991)].
- ⁹N. V. Filippov, *Fiz. Plazmy* **9**, 25 (1983) [*Sov. J. Plasma Phys.* **9**, 14 (1983)].
- ¹⁰J. W. Mather, *Phys. Fluids* **7**, 528 (1964).
- ¹¹A. Bernard *et al.*, in *Proc. Seventh European Conf. Contr. Fusion and Plasma Phys.*, Vol. 1, Lausanne, 1975, p. 60.
- ¹²A. V. Batyunin, A. N. Bulatov, V. D. Vikharev *et al.*, *Fiz. Plazmy* **16**, 1027 (1990) [*Sov. J. Plasma Phys.* **16**, 597 (1990)].
- ¹³K. N. Koshlev and N. R. Pereira, *J. Appl. Phys.* **69** (10), R21 (1991).
- ¹⁴R. B. Spielman *et al.*, in *Proceedings Second International Conference on Dense Z-Pinches*, ed. by N. R. Pereira, J. Davis, and N. Rostoker, AIP, Laguna Beach, 1989, p. 3.
- ¹⁵B. A. Trubnikov, in *Plasma Physics and the Problem of Controlled Thermonuclear Reactions*, Vol. 1, ed. by M. A. Leontovich [in Russian] (Izd-vo Akad. Nauk SSSR, Moscow, 1958).
- ¹⁶N. V. Filipov, T. I. Filipova, and V. P. Vinogradov, *Nucl. Fusion Suppl.* **2**, 577 (1962).
- ¹⁷A. C. Kolb, *Rev. Mod. Phys.* **32** (4), 74 (1960).
- ¹⁸V. F. D'yachenko and V. S. Imshennik, in *Reviews of Plasma Physics*, Vol. 8, ed. by M. A. Leontovich, Consultants Bureau, New York (1980).
- ¹⁹V. S. Imshennik *et al.*, in *Proc. Conference on Plasma Physics and Contr. Nuclear Fus. Res.*, Vol. 2, London, 1985, p. 561.
- ²⁰A. I. Morozov and A. P. Shubin, *Zh. Éksp. Teor. Fiz.* **46**, 710 (1964) [*Sov. Phys. JETP* **19**, 484 (1964)].
- ²¹V. I. Bryzgalov and A. I. Morozov, *Zh. Éksp. Teor. Fiz.* **49**, 1789 (1965) [*Sov. Phys. JETP* **22**, 1223 (1965)].
- ²²A. A. Chernov and V. V. Yan'kov, *Fiz. Plazmy* **8**, 931 (1982) [*Sov. J. Plasma Phys.* **8**, 522 (1982)].
- ²³A. S. Kingsep, K. V. Chukbar, and V. V. Yan'kov, in *Reviews of Plasma Physics*, Vol. 16, ed. by B. B. Kadomtsev, Consultants Bureau, New York (1990).
- ²⁴K. N. Koshlev, V. I. Krauz, N. G. Reshetnyak *et al.*, *Fiz. Plazmy* **15**, 1068 (1989) [*Sov. J. Plasma Phys.* **15**, 619 (1989)].
- ²⁵T. Pizarzyk, A. A. Rupasov, G. S. Sarkisov, and A. S. Shikanov, *J. Sov. Laser Research* **11**, 1 (1990); Preprint No. 135 [in Russian] (*Fiz. Inst. Akad. Nauk, Moscow*, 1989).
- ²⁶A. Raven, P. T. Rumsby, J. A. Stamper *et al.*, *Appl. Phys. Lett.* **35**, 526 (1979).
- ²⁷M. D. J. Burgess, B. Luther-Davies, and K. A. Nugent, *Phys. Fluids* **28**, 2286 (1985).
- ²⁸V. Yu. Bychenkov, Yu. S. Kas'yanov, G. S. Sarkisov, and V. T. Tikhonchuk, *Pis'ma Zh. Éksp. Teor. Fiz.* **58**, 182 (1993) [*JETP Lett.* **58**, 184 (1993)].
- ²⁹Yu. S. Kas'yanov, G. S. Sarkisov, and A. S. Shikanov, *Prib. Tekh. Éksp.* (6), 137 (1994).
- ³⁰S. Czekaj, A. Kasperczuk, R. Miklaszewski *et al.*, *Plasma Phys. and Contr. Fusion* **31**, 587 (1989).
- ³¹V. A. Veretennikov, A. E. Gureĭ, S. N. Polukhin *et al.*, *Fiz. Plazmy* **16**, 818 (1990) [*Sov. J. Plasma Phys.* **16**, 475 (1990)].
- ³²A. V. Brannitskii, V. D. Vikharev, A. G. Kasimov *et al.*, *Fiz. Plazmy* **18**, 1131 (1992) [*Sov. J. Plasma Phys.* **18**, 588 (1992)].
- ³³A. Kasperczuk, M. Paduch, L. Pokora, and Z. Wereszczynski, *J. Techn. Phys.* **19**, 137 (1978).
- ³⁴E. G. Gamali and V. T. Tikhonchuk, *Fiz. Plazmy* **13**, 1527 (1987) [*Sov. J. Plasma Phys.* **13**, 880 (1987)].
- ³⁵Yu. S. Kas'yanov, G. S. Sarkisov, and A. S. Shikanov, *Pis'ma Zh. Éksp. Teor. Fiz.* **58**, 799 (1993) [*JETP Lett.* **58**, 745 (1993)].
- ³⁶Yu. S. Kas'yanov, G. S. Sarkisov, and A. S. Shikanov, *Prib. Tekh. Eksp.* (6), 146 (1994).
- ³⁷S. K. Zhdanov and B. A. Trubnikov, *Zh. Éksp. Teor. Fiz.* **90**, 1380 (1986) [*Sov. Phys. JETP* **63**, 809 (1986)].
- ³⁸G. S. Sarkisov, B. Etlicher, C. Rouille, and S. Attelan, Preprint LPMI 298, Ecole Polytechnique, Palaiseau, France (1994).
- ³⁹P. M. Bellan, *Phys. Rev. Lett.* **69**, 3515 (1992).
- ⁴⁰P. F. Ottinger, S. A. Goldstein, and R. A. Meger, *J. Appl. Phys.* **56**, 774 (1984).
- ⁴¹R. A. Meger, R. J. Commisso, G. Cooperstein, and S. A. Goldstein, *Appl. Phys. Lett.* **42**, 1045 (1983).
- ⁴²K. V. Chukbar and V. V. Yan'kov, *Zh. Tekh. Fiz.* **58**, 2130 (1988) [*Sov. Phys. Tech. Phys.* **33**, 1293 (1988)].
- ⁴³R. J. Mason, P. L. Aurer, R. N. Sudan *et al.*, Preprint LA-UR-92-1409, Ithaca (1992).
- ⁴⁴A. S. Chuvatin, B. Etlicher, N. S. Edison, and C. Rouille, *Rev. Sci. Instrum.* **64**, 2267 (1993).
- ⁴⁵P. V. Satorov, *Pis'ma Zh. Éksp. Teor. Fiz.* **56**, 614 (1992) [*JETP Lett.* **56**, 599 (1992)].
- ⁴⁶M. G. Haines, *Proc. Phys. Soc.* **74**, 576 (1959).

Translated by Julian B. Barbour